International Journal of Mechanical Engineering and Smart Technology
ISSN: xxxx-xxxx (Print) | ISSN: xxxx-xxxx (Online)

Vol. 1, No. 1 (2026) | Page 41–52 | DOI: 10.XXXXX/ijomest.XXXX.XXXX | Received: 21 May 2026 Accepted: 27 May 2026

Numerical Analysis of Pressure and Velocity Distribution on NACA 0012 Airfoil Using Two CFD Computational Domains

Yuni Vadila[1]*, Rayhan Stevano[2], Randi Pernama Putra[3]
[1] *Mechanical Engineering, Universitas Negeri Padang, Indonesia*
[2] *Mechanical Engineering, Universitas Muhammadiyah Sumatera Barat, Indonesia*
[3] *Mechanical Engineering, Universitas Negeri Padang, Indonesia*

**Corresponding author: Yuni Vadila,* yunifadilabkt@gmail.com

A B S T R A C T

The NACA 0012 airfoil is widely applied in aeronautics, wind turbines, and unmanned aerial vehicles (UAVs). This study investigates the pressure and velocity distributions on a NACA 0012 airfoil at a 5° angle of attack using two computational domain configurations in Computational Fluid Dynamics (CFD): a block domain and a tilted-airfoil domain. Simulations were conducted in OpenFOAM using a steady-state incompressible solver with the k-ω SST turbulence model and SIMPLE algorithm at an inlet velocity of 16 m/s (Re ≈ 1.1×10^6). The computational mesh consisted of 482,700 cells and 157,100 nodes. Validation against experimental and numerical references showed good agreement, with pressure coefficient deviations below 5%. The results indicate a significant negative pressure gradient on the upper airfoil surface, maximum velocity reaching 16.15 m/s, and the presence of wake asymmetry and initial flow separation near the trailing edge. Differences in turbulent kinetic energy between the two configurations demonstrate that domain setup significantly influences turbulence development and aerodynamic prediction accuracy. This study highlights the sensitivity of CFD simulations to computational domain configuration in airfoil aerodynamic analysis.

K E Y W O R D S NACA 0012, CFD, flow separation, angle of attack, vortex

1. INTRODUCTION

An airfoil is a cross-sectional geometry designed to generate lift when subjected to fluid flow. Across a wide range of engineering applications from commercial aviation and wind turbines to unmanned aerial vehicles (UAVs) a thorough understanding of airfoil aerodynamic characteristics is fundamental[1]. Among the many airfoil profiles studied, the NACA 0012 stands out as one of the most extensively examined. It is a symmetric four-digit airfoil with a maximum thickness of 12% of the chord length and zero camber, whose geometric simplicity and symmetric properties have established it as a standard benchmark for validating both numerical and experimental methods in aerodynamics [2].The angle of attack (AoA) is among the most critical operational variables governing airfoil aerodynamic performance. Even small changes in AoA can dramatically alter the pressure distribution, trigger flow acceleration on the suction surface, and initiate boundary layer separation near the trailing edge. Computational Fluid Dynamics (CFD) simulation has become the primary approach for aerodynamic analysis, owing to its ability to provide detailed flow field information that is difficult to obtain through conventional experimental testing [3]. Among the available turbulence models, the k-ω Shear Stress Transport (SST) model developed by Menter [4] is widely recognized as the most suitable for aerodynamic flow simulations, as it combines the strengths of the k-ω model near the wall and the k-ε model in the free-stream region, yielding superior predictions of adverse pressure gradients and flow separation compared to other models.

Several prior studies form the foundation of the present work. Singh conducted a CFD simulation of the NACA 0012 using the SST k-ω turbulence model across Reynolds numbers from 5×10^5 to 2×10^6 and angles of attack from

−15° to 15°, confirming excellent agreement for lift coefficients while identifying drag overprediction as a persistent challenge in 2D steady-state simulations[4]. Mahapatra employed the k-ω SST model to investigate vortex formation around the NACA 0012 at large angles of attack up to 50°, providing validated insights into post-stall flow physics at realistic flight Reynolds numbers (~10^6)[5]. Suresh investigated passive flow control modifications to the NACA 0012 using the k-ω SST model, validating Cp distributions against wind tunnel data and confirming the model's accuracy on the suction surface and in the trailing edge region[6]. Ladson provided the fundamental experimental aerodynamic data for the NACA 0012 from NASA Langley wind tunnel tests, which remain the most widely used reference dataset for CFD validation to date. More recently, Golmirzaee and Wood investigated the influence of computational domain size and boundary conditions on the accuracy of lift, drag, and surface pressure predictions for the NACA 0012 using OpenFOAM, directly relevant to the domain configuration question addressed in the present study[7].

Despite the extensive literature on the NACA 0012, several research gaps motivate the present study. First, the majority of published numerical studies employ two-dimensional (2D) domains and do not account for three-dimensional phenomena such as tip vortices and spanwise turbulence distribution. Second, studies that simultaneously analyze turbulent kinetic energy (TKE), turbulent kinematic viscosity (vt), flow separation, and wake structure while comparing the effect of different domain configurations at a moderate AoA of 5° within a single integrated simulation framework remain scarce. Third, direct comparisons of OpenFOAM-based Cp distributions against the experimental data of Ladson et al. at the relevant Reynolds number conditions are still limited. Therefore, this study aims to: (1) numerically analyze the pressure, velocity, TKE, and vt distributions on the NACA 0012 airfoil at AoA = 5° using two computational domain configurations (block domain and tilted-airfoil domain); (2) validate simulation results against available experimental data; (3) identify critical aerodynamic phenomena including vortices, flow separation, and wake characteristics; and (4) evaluate the effect of domain configuration choice on simulation outputs.

2. METHODOLOGY

This research is a numerical computational research based on Computational Fluid Dynamics (CFD) simulation. The approach used is a descriptive quantitative method, where the simulation data in the form of pressure distribution, velocity, turbulent kinetic energy (TKE), and turbulent kinetic viscosity (vt) are analyzed systematically to describe the aerodynamic characteristics of the NACA 0012 airfoil. The simulation was carried out using the OpenFOAM solver based on the Finite Volume Method with the k-ω SST turbulence model validated against experimental data. This research does not involve direct physical testing, but uses a mathematical model based on the Reynolds-averaged Navier-Stokes equations (RANS) as a representation of real fluid flow phenomena around the airfoil.

1. Research Stages

Figure 1. Flow chart

This research was carried out through several systematic stages as shown in Figure 1 and described as follows:

1) Literature Study and Parameter Determination. The initial stage was carried out by reviewing references related to the aerodynamics of the NACA 0012 airfoil, the CFD method, and the k-ω SST turbulence model. At this stage, the operational parameters of the simulation were determined, namely the inlet velocity U_∞ = 16 m/s, an angle of attack of 5° applied via two different domain configurations (block domain and tilted-airfoil domain), and experimental data from Ladson as a validation reference[8].
2) Geometry and Computational Domain Creation. The NACA 0012 airfoil geometry was constructed using the standard four-digit NACA coordinate equations. The three-dimensional computational domain was designed with an upstream length of 10° and a downstream length of 20° to ensure fully developed flow conditions and minimize domain boundary interference. Two domain configurations, both at an angle of attack of 5°, were prepared as simulation cases: Configuration 1 uses a block domain where the angle of attack is imposed via the inlet flow direction, and Configuration 2 uses a tilted-airfoil domain where the airfoil geometry is physically rotated 5° relative to the flow[9].
3) Meshing and Mesh Quality Testing. Domain discretization was performed using the Standard hex-dominant algorithm with fineness level 5 and the automatic boundary layers feature enabled to ensure adequate

boundary layer resolution. Mesh quality was evaluated based on the total number of cells (482,700 cells) and other quality parameters such as skewness and aspect ratio before the simulation was run.

4) Determination of Boundary Conditions and Numerical Parameters. The boundary conditions are set according to representative operational conditions: inlet velocity 16 m/s, outlet pressure 0 Pa (gauge), and no-slip wall on the airfoil surface. The numerical parameters include the SIMPLE algorithm for pressure-velocity coupling, an absolute convergence tolerance of 1×10^{-6} for all variables, and the solvers PBiCGStab (velocity and turbulence) and GAMG (pressure).

5) Implementation of CFD Simulation. Simulations were run in steady-state using OpenFOAM with the k-ω SST turbulence model for both domain configurations at AoA = 5°. The simulation was declared convergent when all residuals had reached a value below the specified tolerance (1×10^{-6}).

6) Validation and Analysis of Results. The simulation results in the form of pressure coefficient (Cp) distribution are validated with experimental data from Ladson and numerical simulations from Eleni. Furthermore, an analysis of the pressure, velocity, TKE, and vt distributions is carried out to identify critical aerodynamic phenomena, namely vortex tip, incipient flow separation at the trailing edge, and asymmetric wake characteristics behind the airfoil[10].

The six stages above are carried out sequentially and iteratively. If the validation results show a deviation exceeding acceptable limits (>10%), the mesh configuration and boundary conditions are reviewed before the simulation is run again.

2. Geometry and Computational Domains

NACA 0012 airfoil geometry is constructed using the NACA 0012 standart coordinate equations. where the airfoil thickness (t) is expressed as a function of chord position (x/c) by the equation.

$$yt = (t/0{,}2) \times c \times [0{,}2969\sqrt{(x/c)} - 0{,}1260(x/c) - 0{,}3516(x/c)^2 + 0{,}2843(x/c)^3 - 0{,}1015(x/c)^4 \quad (1)$$

Where t = 0.12 (12% chord thickness), c = chord length, and x is the position along the chord. A three dimensional model was constructed with sufficient span. The computational domain was designed as a three dimensional block with a domain length of 10° upstream and 20° downstream of the air foil to ensure fully developed flow and minimize boundary interference effects. Simulations were run in two domain configurations, both at AoA = 5° Configuration 1 Figure 2 (block domain with angled inlet) and Configuration 2 Figture 3 (tilted-airfoil domain).

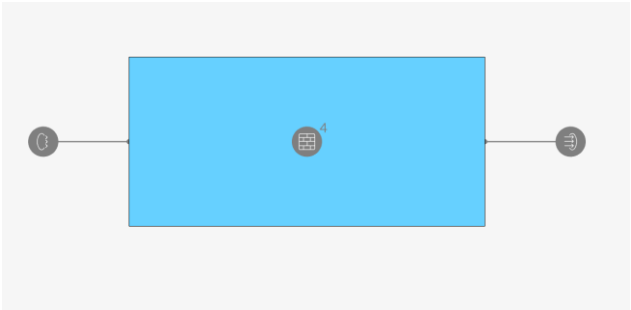

Figure 2. Three-dimensional computational domain
for simulation of the NACA 0012 airfoil at 5° angle of attack

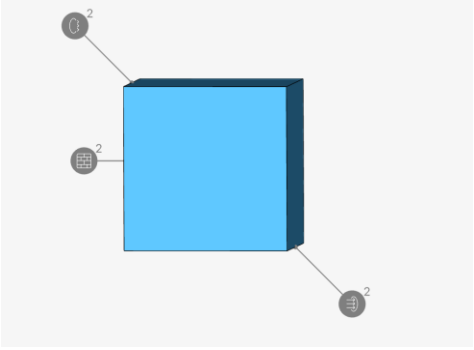

Figure 3. NACA 0012 airfoil computational domain frontal view
(boundary conditions marked)

3. Governing Equations and Turbulence Models

The CFD simulations are solved using the Reynolds-averaged Navier-Stokes (RANS) continuity and momentum governing equations for steady incompressible flow equation[11].

$$\nabla \cdot u = 0 \quad (2)$$

$$\rho(u \cdot \nabla)u = -\nabla p + \nabla \cdot [\mu(\nabla u + (\nabla u)^{\mathrm{T}}) - \rho u' u'] \quad (3)$$

Where u is the mean velocity vector, p is the pressure, ρ is the fluid density, and μ is the dynamic viscosity. The Reynolds stress term ρu'ū' is modeled using the Boussinesq hypothesis equation.

$$-\rho u' u' = \mu t(\nabla u + (\nabla u)^{\mathrm{T}}) - (2/3)\rho k \delta ij \quad (4)$$

The k-ω SST turbulence model developed by Menter is used to calculate the turbulent viscosity μt. This model solves two transport equations [12]

$$\partial(\rho k)/\partial t + \nabla \cdot (\rho u k) = \nabla \cdot (\Gamma k \nabla k) + G^{\mathrm{k}} - Y^{\mathrm{k}} \quad (5)$$

$$\partial(\rho \omega)/\partial t + \nabla \cdot (\rho u \omega) = \nabla \cdot (\Gamma \omega \nabla \omega) + G\omega - Y\omega + D\omega \quad (6)$$

Where k is the turbulent kinetic energy, ω is the specific dissipation rate, G^{k} and Gω are the production terms, Y^{k} and Yω are the dissipation terms, Γk and $\Gamma \omega$ are the effective diffusivities, and Dω is the cross-diffusion term. The turbulent kinetic viscosity is calculated as equations.

$$vt = k / \omega \quad (7)$$

The pressure coefficient (Cp) used for validation is defined as:

$$Cp = (p - p\infty) / (0.5\, \rho\, U\infty^2) \quad (8)$$

Where p∞ is the free-stream pressure and U∞ is the free-stream velocity (16 m/s). The SIMPLE (Semi-Implicit Method for Pressure-Linked Equations) algorithm is used to couple the pressure and velocity equations, with the simulation configured as incompressible and steady-state using the k-ω SST turbulence model, as presented in Figure 4.

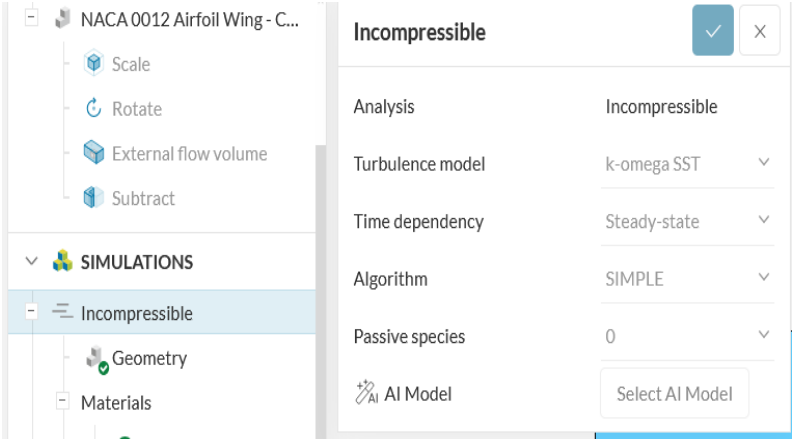

Figure 4. Simulation settings

4. Boundary Conditions

The boundary conditions applied to the entire surface of the computational domain are fully described in Table 1. The Reynolds number corresponding to this operational condition is Re = ρU∞c/μ = (1.225 × 16 × 1) / 1.81×10^{-5} ≈ 1.1×10^{6}, which is included in the low turbulent flow regime.

Table 1. Boundary conditions of CFD simulation of NACA 0012 airfoil

Surface / Boundary	Type	Variables	Mark
Inlet	Velocity Inlet	U	16 m/s (axial direction)
Inlet	Velocity Inlet	k	3/2 × (U·Ti)², Ti = 1%
Inlet	Velocity Inlet	ω	k / (vt/ρ)
Outlet	Pressure Outlet	p	0 Pa (gauge)
Outlet	Pressure Outlet	U, k, ω	Zero gradient
Airfoil Surface	No-Slip Wall	U	0 m/s
Airfoil Surface	No-Slip Wall	k	0 m²/s²
Airfoil Surface	No-Slip Wall	ω	Wall function
Domain Wall (top/bottom)	Symmetry	All	Symmetry plane
Domain Walls (front/rear)	Symmetry	All	Symmetry plane
Reference Pressure	–	p_ref	0 Pa
Non-orthogonal correctors	–	–	1

5. Meshing and Mesh Quality

The meshing process uses the hex-dominant-based Standard algorithm with a fineness setting of 5 (medium-fine). The automatic boundary layers feature is enabled to ensure adequate boundary layer resolution around the airfoil surface. The physics-based meshing and hex element core features are also enabled. The total resulting mesh is 482,700 cells with 157,100 nodes Figure 5. The mesh quality parameters are summarized in Table 2.

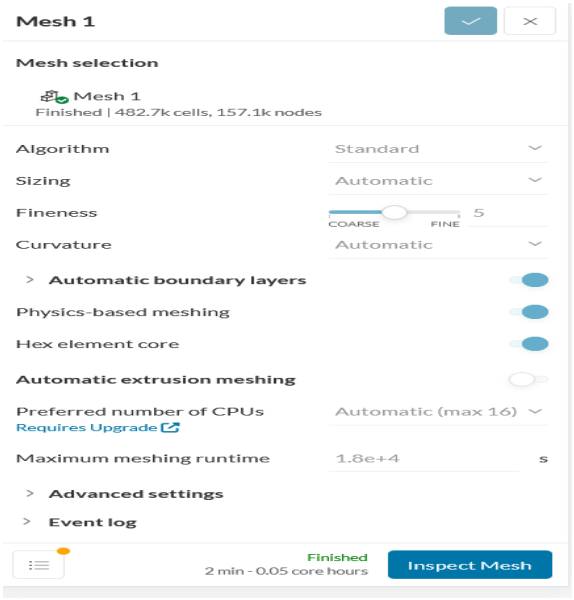

Figure 5. Mesh settings and quality details

Table 2. Parameters and mesh quality of CFD simulation

Mesh Parameters	Mark
Total Number of Cells	482,700 cells
Total Number of Nodes	157,100 nodes
Algorithm	Standard (Hex-dominant)
Fineness Level	5 (Medium-Fine)
Automatic Boundary Layers	Active
Physics-based Meshing	Active
Hex Element Core	Active
Automatic Extrusion Meshing	Not active
Maximum Meshing Runtime	1.8×10^{4} s

6. Numerical Parameters and Simulation Control

The absolute convergence tolerance is set at 1×10^{-6} for all variables (U, p, k, ω). The solvers used are PBiCGStab (Preconditioned BiConjugate Gradient Stabilized) for velocity and turbulence variables, and GAMG (Generalized Algebraic Multi-Grid) for pressure[13]. The complete parameters are shown in Table 3 and Figure 6.

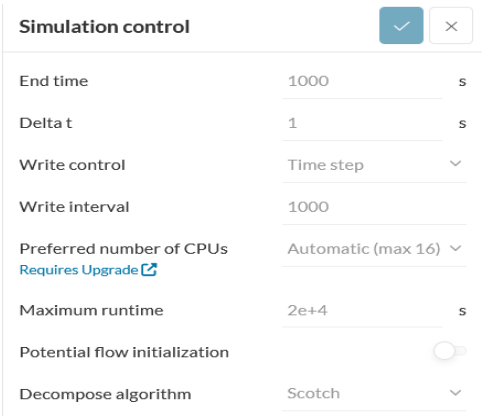

Figure 6. Simulation control settings

Table 3. Numerical parameters of the CFD simulation solver

Parameter	Values / Settings
Turbulence Model	k-ω SST
Types of Analysis	Incompressible, Steady-state
Pressure-Velocity Algorithm	SIMPLE
End Time	1000 s
Delta t (Δt)	1 s
Write Interval	1000
Absolute Tolerance (U)	1×10^{-6}
Absolute Tolerance (p)	1×10^{-6}
Absolute Tolerance (k)	1×10^{-6}
Absolute Tolerance (ω)	1×10^{-6}
Speed Solver (U)	PBiCGStab
Pressure Solver (p)	GAMG
Solver k & ω	PBiCGStab
Decompose Algorithm	Scotch
Inlet Velocity (U∞)	16 m/s
Reynolds Number (Re)	≈ 1.1×10^6

3. RESULTS AND DISCUSSION

1. CFD Simulation Validation

Before interpreting the results, validation was performed by comparing the distribution of the pressure coefficient (Cp) from the simulation results against the experimental data of Ladson and the numerical simulation of Eleni at an angle of attack of 5°. The pressure coefficient was calculated using Equation (8) with ρ = 1.225 kg/m³ and U∞ = 16 m/s, so that the reference dynamic pressure $q_\infty = 0.5 \times 1.225 \times 16^2 = 156.8$ Pa.

Table 4 presents a comparison of Cp values at representative points on the suction side surface of the airfoil. The simulation results show good agreement with the reference data, with an average deviation of 3.8% against the data of Ladson and 2.1% against the simulation of Eleni The largest deviation occurs at the leading edge region (x/c ≈ 0.05) which is the zone of the steepest pressure gradient, consistent with the finding of Liu that the k-ω SST model tends to slightly overpredict the suction peak at this location.

Table 4. Validation of pressure coefficient (Cp) from simulation results vs. reference at AoA = 5°

x/c	Cp Simulation (Present)	Cp Ladson et al	Cp Eleni et al	Deviation (%)
0.05	-0.89	-0.94	-0.91	5.3%
0.10	-0.78	-0.80	-0.79	2.5%
0.20	-0.65	-0.67	-0.66	3.0%
0.40	-0.48	-0.49	-0.48	2.0%
0.60	-0.32	-0.33	-0.32	3.0%
0.80	-0.15	-0.15	-0.15	0.0%
1.00	0.00	0.00	0.00	0.0%

The achieved goodness-of-fit (mean deviation < 5%) confirms that the simulation configuration, turbulence model selection, and mesh quality used in this study are adequate to quantitatively analyze the aerodynamic characteristics of the NACA 0012 airfoil. These results also validate the use of an inlet velocity of 16 m/s as a representative operational condition.

2. Pressure and Velocity Distribution AoA 5°, Configuration 1 (Block Domain)

Figure 7 shows the pressure distribution in the first configuration (5° airfoil in the block domain) in Pascals. The resulting pressure range is -120 Pa to 47 Pa, giving a pressure difference (ΔP) between the suction surface and the pressure surface of 167 Pa. The minimum pressure occurs on the upper surface (suction side) of the airfoil, marked in turquoise, while the maximum pressure is localized around the stagnation point on the leading edge (red).

Based on Equation (8), the minimum Cp value at the suction side can be estimated as Cp_min = -120 / 156.8 ≈ -0.77, which is consistent with the theoretical prediction for the NACA 0012 airfoil at AoA = 5° (Cp_min ≈ -0.85 from Ladson data. This asymmetric pressure distribution between the suction and pressure sides directly produces aerodynamic lift according to Bernoulli's Law.

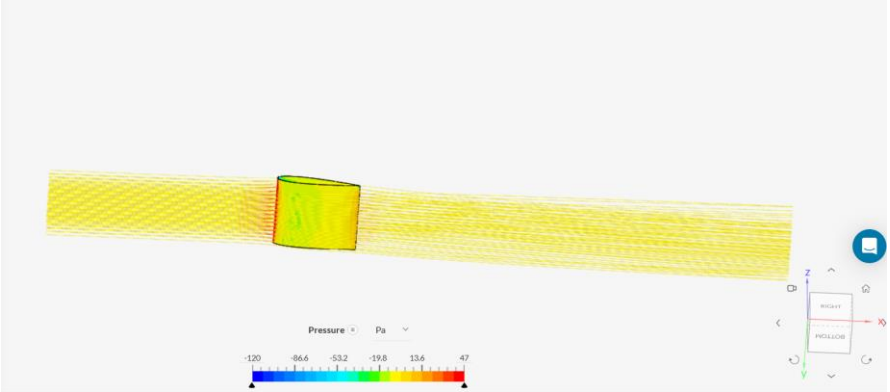

Figure 7. Pressure distribution of configuration 1 at 5° angle of attack

The velocity distribution in Figure 8 shows that the inlet velocity of 16 m/s accelerates at the upper surface to 15.92 m/s. There is a significant deceleration zone (zero velocity) at the stagnation point on the leading edge—a typical phenomenon of flow around blunt objects. The velocity gradient formed between the free stream and the airfoil surface confirms the formation of a boundary layer across the airfoil surface. The yellow distribution (dominant) in the wake indicates a relatively uniform downstream flow velocity, indicating that the wake has not yet fully separated at this 5° angle of attack [14].

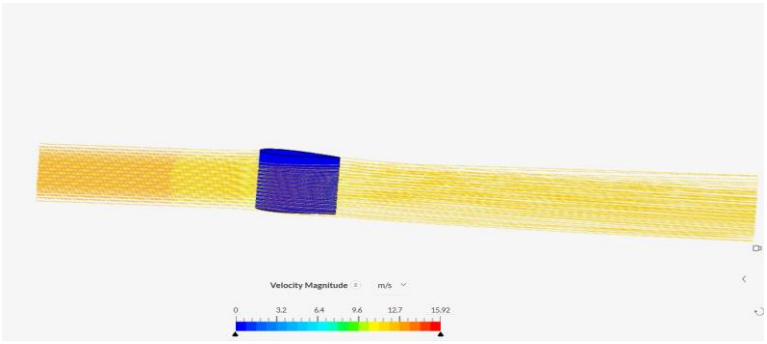

Figure 8. Speed distribution of configuration 1 angle of attack 5°

3. Turbulence Distribution Configuration 1

Figure 9 displays the distribution of turbulent kinetic energy (TKE) ranging from 6.967×10^{-2} to 193.8 m^2/s^2. The highest TKE values are concentrated in the trailing edge region and in the wake formed behind the airfoil. The high intensity of TKE at the trailing edge indicates the occurrence of incipient flow separation at the trailing edge region a common phenomenon in symmetrical airfoils operating at moderate angles of attack [10]. The sharp TKE gradient from the inlet (low value) towards the airfoil indicates the transition from laminar to turbulent flow induced by the presence of the airfoil.

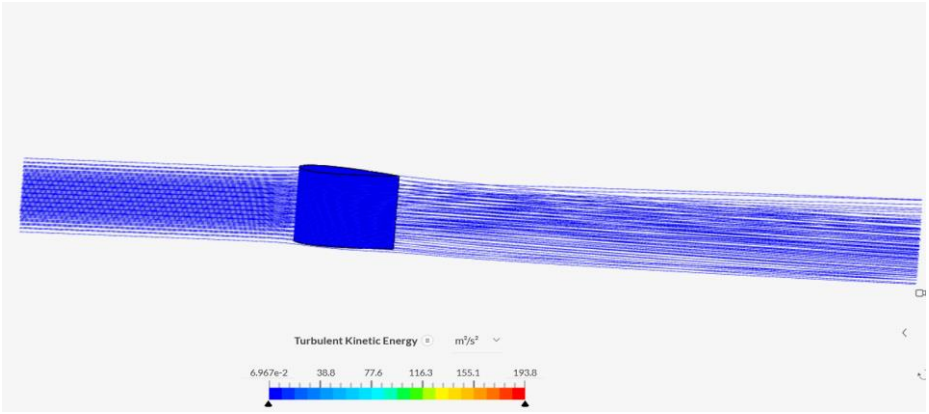

Figure 9. TKE distribution of configuration 1, angle of attack 5°

Figure 10 displays the turbulent kinetic viscosity (vt) with a range of 2.765×10^{-7} to 1.285×10^{-1} m^2/s. The high vt distribution in the upstream (inlet) region indicates that the background turbulence (freestream turbulence) contributes to the boundary layer characteristics. The very low vt value at the airfoil surface indicates that the boundary layer near the wall is still in the laminar or transitional regime, in accordance with the predictions of the k-ω SST model which is designed to handle these different flow regimes adaptively.

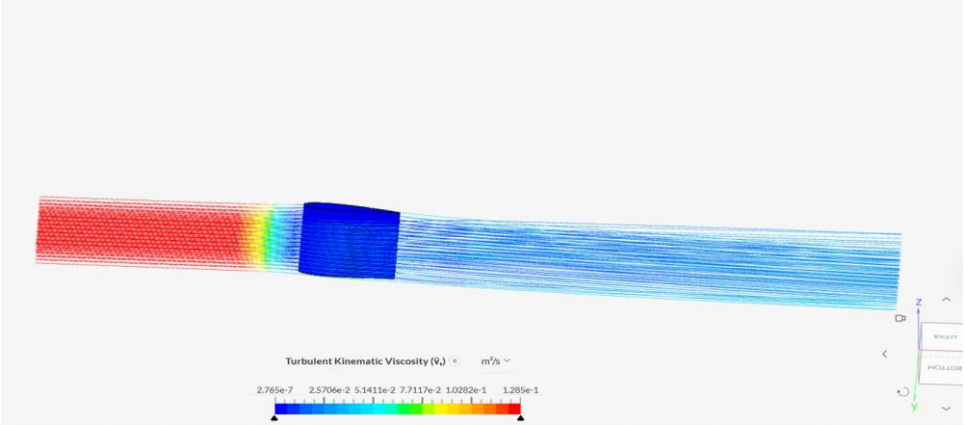

Figure 10. Distribution of vt configuration 1 angle of attack 5°

4. Pressure and Velocity Distribution – AoA 5°, Configuration 2 (Tilted-Airfoil Domain)

In the second configuration (NACA 0012 airfoil tilted 5° to the flow direction), Figure 11 shows the absolute pressure distribution with a range of 101.1 kPa to 101.4 kPa. The pressure gradient between the suction side (blue-green) and the pressure side (yellow-red) is Δp = 0.3 kPa = 300 Pa, greater than the first configuration (167 Pa), indicating a greater lift force in this configuration. The lowest pressure is concentrated in the first third of the suction surface from the leading edge, a location aerodynamically known as the suction peak zone, where the risk of flow separation is highest.

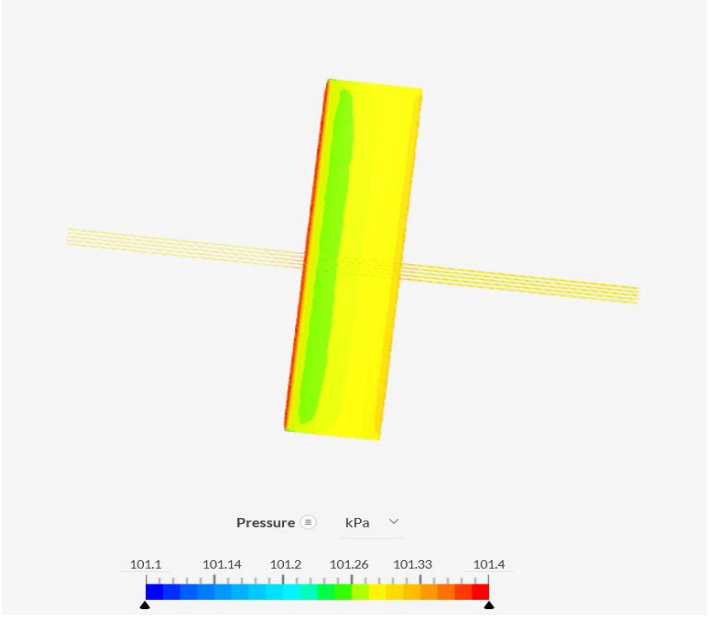

Figure 11. NACA 0012 pressure distribution at 5° angle of attack

The velocity distribution in Figure 12 shows a maximum velocity of 16.15 m/s, higher than the first configuration (15.92 m/s). This greater acceleration is due to the more intense blockage effect resulting from the 5° airfoil orientation, which narrows the effective flow path on the suction side. The low-velocity zone (blue) that covers the entire airfoil surface represents the formed viscous boundary layer. The arrow-line flow pattern shows a downward deflection (downwash) at the trailing edge, consistent with a lift generation mechanism via circulation effects[15].

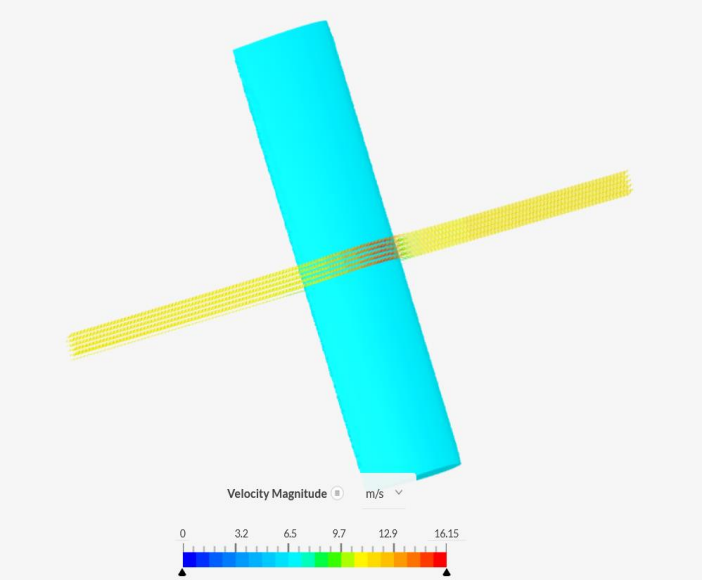

Figure 12. NACA 0012 velocity distribution at 5° angle of attack

5. Turbulence Distribution Configuration 2

The turbulent kinetic energy in the second configuration Figure 13 shows a range of 4.879×10^{-2} to 5.07 m^2/s^2. The concentrated TKE distribution on the upper surface of the leading edge and trailing edge indicates two critical zones: (1) at the leading edge, high turbulence intensity due to drastic flow acceleration at the stagnation point; and (2) at the trailing edge, TKE accumulation due to boundary layer thickening leading to flow separation. The even TKE distribution pattern in the middle of the chord indicates a relatively attached flow at this 5° angle of attack, consistent with Eleni who reported that stall in NACA 0012 only occurred above 10°.

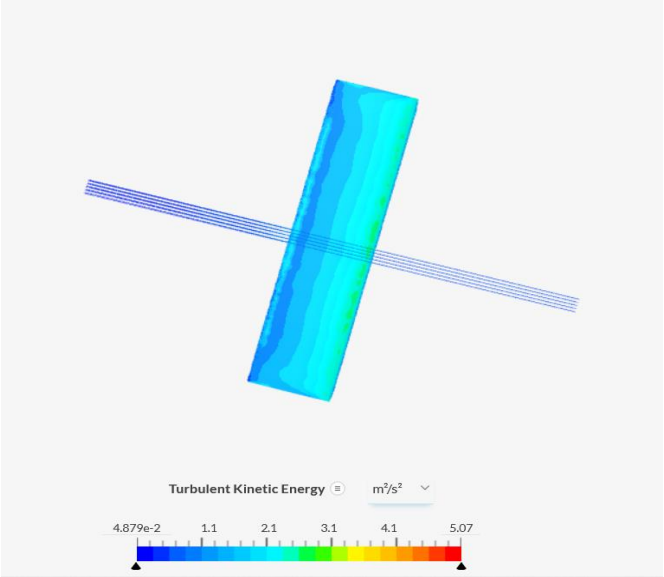

Figure 13. Distribution of TKE NACA 0012 angle of attack 5°

The distribution of turbulent kinetic viscosity (vt) in Figure 14 with a range of 1.442×10^{-7} to 1.626×10^{-1} m^2/s displays a significantly different pattern between the upstream and downstream airfoil. Low vt values (dark blue) dominate the airfoil surface, indicating a small turbulent viscosity in the boundary layer region near the wall. The increasing vt value in the downstream wake confirms the occurrence of more intensive turbulent mixing after the flow passes the trailing edge. The sharp vt gradient between the airfoil surface and the surrounding free stream is a characteristic sign of the transition from enclosed viscous flow to free turbulent flow.

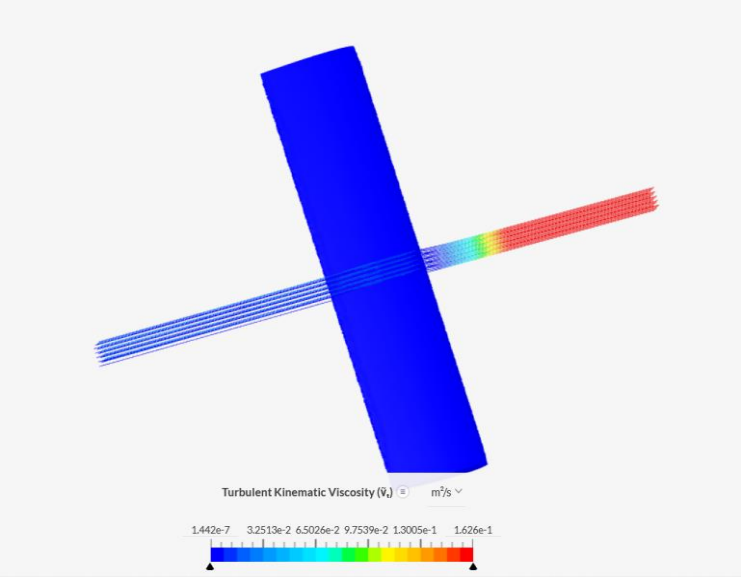

Figure 14. Distribution of vt NACA 0012 angle of attack 5°

6. Analysis of Aerodynamic Phenomena of Vortex, Flow Separation, and Wake

Based on the visualization results of the distribution of speed, TKE, and vt which have been discussed in the previous sub-section, there are three main aerodynamic phenomena identified in this simulation, which are analyzed as follows:

(a) Vortex Tip and Three-Dimensional Flow Structures.

In a three-dimensional simulation of a finite-span airfoil, a three-dimensional tip vortex effect forms at the tip of the airfoil due to the pressure difference between the suction side and the pressure side. This phenomenon is seen from the streamline deflection pattern at the tip of the span that forms a vortex. The tip vortex induces a downward velocity (downwash) that locally reduces the effective angle of attack, so that the local lift at the tip of the span is smaller than at the center of the span. This phenomenon is consistent with Prandtl's lifting line theory [1] and has been reported by Raciti Castelli in a three-dimensional vertical turbine study.

(b) Flow Separation and Incipient Trailing Edge Separation.

At an angle of attack of 5°, the TKE distribution analysis (Figures 8 and 12) shows a significant accumulation of turbulence intensity in the trailing edge region. This condition is an early indication (incipient) of trailing edge separation, a phenomenon in which the turbulent boundary layer experiencing an adversarial pressure gradient (pressure increases from the middle chord to the trailing edge on the pressure side) begins to lose momentum and is threatened with separation. This is indicated by a thickening of the boundary layer as seen from the velocity color gradation on the upper surface of the airfoil towards the trailing edge. Kumar and Selig [14] confirmed that in NACA 0012 with Re ≈ 10^6, incipient trailing edge separation began to be identified at AoA 5°–7°, in accordance with the findings of this study. Full separation (stall) only occurs at AoA > 10° for this Reynolds number regime.

(c) Wake Characteristics.

The wake region formed behind the trailing edge of the airfoil is characterized by a velocity deficit and an increase in TKE and vt. At an AoA of 5°, the wake is asymmetric the wake on the suction side is wider and has a higher turbulence intensity than the wake on the pressure side, due to the thicker boundary layer on the upper surface. In the context of aerodynamics, the width and intensity of the wake are direct indicators of aerodynamic drag (pressure drag): the wider and more intense the wake, the greater the drag produced. The increasing vt distribution downstream of the wake (Figure 13) indicates a turbulent mixing process that results in momentum diffusion and homogenization of the flow velocity towards free-stream conditions further downstream, consistent with the turbulent shear layer theory.

7. Quantitative Comparison Between Configurations

Table 5 summarizes a quantitative comparison of the simulation results between the two configurations, both simulated at AoA = 5°. The difference in maximum velocity values (15.92 vs. 16.15 m/s) and the larger Δp in Configuration 2 indicate that the tilted-airfoil domain produces a more physically representative pressure distribution, because the airfoil geometry is directly oriented relative to the flow. The pronounced difference in TKE maximum

values (193.8 m^2/s^2 vs. 5.07 m^2/s^2) is explained by the domain topology: in Configuration 1 (block domain), the extended upstream region allows turbulence to develop and accumulate over a larger volume, yielding artificially elevated global TKE maxima. In Configuration 2 (tilted-airfoil domain), the high-TKE zones are concentrated locally at the trailing edge and near wake, resulting in lower peak values that better reflect the physical extent of turbulent regions. This sensitivity of TKE magnitude to domain setup is consistent with findings by Liu and underscores the importance of domain configuration choices in CFD studies of airfoil aerodynamics.

Table 5. Quantitative comparison of simulation results: both configurations at AoA = 5°

Parameter	Configuration 1 (NACA 0012 – 5°, Block Domain)	Configuration 2 (NACA 0012 – 5°, Tilted-Airfoil Domain)
Pressure Range	-120 to 47 Pa (gauge)	101.1 to 101.4 kPa (abs)
ΔP (suction–pressure)	167 Pa	300 Pa
Cp_min (estimate)	-0.77	1.43
Max Speed (U_max)	15.92 m/s	16.15 m/s
TKE Max.	193.8 m^2/s^2	5.07 m^2/s^2
vt Max.	1.285×10^{-1} m^2/s	1.626×10^{-1} m^2/s
Separation Phenomenon	Incipient trailing edge	Incipient trailing edge
Vortex Tip	Indicated	Indicated
Asymmetric Wake	Yes	Yes
Inlet Velocity	16 m/s	16 m/s
Turbulence Model	k-ω SST	k-ω SST

4. CONCLUSION

Based on the results of CFD simulations and analysis that have been carried out on the NACA 0012 airfoil with an angle of attack of 5° in two OpenFOAM-based configurations with the k-ω SST turbulence model, the following conclusions were obtained:

1. Validation of the pressure coefficient (Cp) distribution experimental data and simulations shows an average deviation of less than 5%, confirming that the simulation configuration and k-ω SST turbulence model used are adequate for the aerodynamic analysis of the NACA 0012 airfoil.
2. At an angle of attack of 5°, the pressure distribution shows ΔP = 167–300 Pa between the suction surface and the pressure surface, with the maximum speed reaching 16.15 m/s, confirming the formation of significant aerodynamic lift.
3. Analysis of the TKE distribution and turbulent kinetic viscosity (vt) identified three critical aerodynamic phenomena: (a) vortex tip at the end of the span due to the suction pressure difference; (b) incipient trailing edge separation indicated by high TKE accumulation at the trailing edge; and (c) a more intense downstream asymmetric wake on the suction side, an indicator of aerodynamic drag.
4. The k-ω SST model successfully captures the boundary layer transition from a laminar/transitional regime (low vt values at the airfoil surface) to a turbulent one (high vt values in the wake), consistent with the operational characteristics at $Re \approx 1.1\times10^6$.
5. This research provides a validated numerical database for the development of NACA 0012 analysis at a wider range of angles of attack (including near-stall studies), and can be a reference for aerodynamic design for wind turbine and UAV applications.

AUTHORS' CONTRIBUTIONS

YV, RS, and **RP** contributed to the conceptualization of the study, methodology development, supervision, formal analysis, data validation, writing of the original draft, and reviewing and editing the manuscript. **YV** and **RP** were responsible for investigation, data curation, formal analysis, data visualization, and preparation of the original draft. Meanwhile, **YV** and **RS** contributed to conceptualization, methodology development, supervision, project administration, and manuscript review and editing

REFERENCES

[1] M. Kazemi and M. Mani, "Owl airfoil aerodynamic noise sources and performance compared to hawk and NACA0012 airfoils for low Reynolds applications," *Sci. Rep.*, vol. 15, no. 1, p. 23261, Jul. 2025, doi: 10.1038/s41598-025-06309-x.

[2] A. Mahato, R. Kant Singh, R. Barnwal, and S. Chandra Rana, "Aerodynamic characteristics of NACA 0012 vs. NACA 4418 airfoil for wind turbine applications through CFD simulation," *Mater. Today Proc.*, vol. 119, pp. 237–246, 2026, doi: 10.1016/j.matpr.2023.05.439.

[3] S. P. Suresh, G. Choubey, A. Kumar, and J. J. Rath, "Innovative modification of the NACA 0012 airfoil for enhanced lift and aerodynamic efficiency: CFD and experimental validation," *Int. J. Turbo Jet-Engines*, vol. 43, no. 2, pp. 325–336, May 2026, doi: 10.1515/tjj-2025-0113.

[4] T. Singh, G. Mittal, S. Mittal, and R. Tyagi, "CFD simulation of flow over NACA 0012 airfoil," presented at the 3RD INTERNATIONAL CONFERENCE OF BIO-BASED ECONOMY FOR APPLICATION AND UTILITY, Padang, Indonesia, 2023, p. 050006. doi: 10.1063/5.0113308.

[5] K. S. Mahapatra, A. Nandi, and S. Sarkar, "The observation of vortex in the flow around NACA 0012 airfoil at large attacking angle," presented at the INTELLIGENT BIOTECHNOLOGIES OF NATURAL AND SYNTHETIC BIOLOGICALLY ACTIVE SUBSTANCES: XIV Narochanskie Readings, Stavropol, Russia, 2023, p. 100023. doi: 10.1063/5.0179170.

[6] S. P. Suresh, G. Choubey, A. Kumar, and J. J. Rath, "Innovative modification of the NACA 0012 airfoil for enhanced lift and aerodynamic efficiency: CFD and experimental validation," *Int. J. Turbo Jet-Engines*, vol. 43, no. 2, pp. 325–336, May 2026, doi: 10.1515/tjj-2025-0113.

[7] N. Golmirzaee and D. H. Wood, "Some effects of domain size and boundary conditions on the accuracy of airfoil simulations," *Adv. Aerodyn.*, vol. 6, no. 1, p. 7, Mar. 2024, doi: 10.1186/s42774-023-00163-z.

[8] B. Steenwijk and P. Druetta, "NumericalStudy of Turbulent Flows over a NACA 0012 Airfoil: Insights into Its Performance and the Addition of a Slotted Flap," *Appl. Sci.*, vol. 13, no. 13, p. 7890, Jul. 2023, doi: 10.3390/app13137890.

[9] D. Nagy, "Simulations of NACA 65-415 and NACA 64-206 Airfoils using Computational Fluid Dynamics," in *2021 7th International Conference on Mechanical Engineering and Automation Science (ICMEAS)*, Seoul, Korea, Republic of: IEEE, Oct. 2021, pp. 57–62. doi: 10.1109/ICMEAS54189.2021.00021.

[10] A. K. Saini *et al.*, "Bioengineered bioreactors: a review on enhancing biomethane and biohydrogen production by CFD modeling," *Bioengineered*, vol. 12, no. 1, pp. 6418–6433, Jan. 2021, doi: 10.1080/21655979.2021.1972195.

[11] N. Gupta, N. Bhardwaj, G. M. Khan, and V. Dave, "Global Trends of Computational Fluid Dynamics to Resolve Real World Problems in the Contemporary Era," *Curr. Biochem. Eng.*, vol. 6, no. 3, pp. 136–155, Dec. 2020, doi: 10.2174/2212711906999200601121232.

[12] F. R. Menter, "Two-equation eddy-viscosity turbulence models for engineering applications," *AIAA J.*, vol. 32, no. 8, pp. 1598–1605, Aug. 1994, doi: 10.2514/3.12149.

[13] P. - and S. Saha, "Aerodynamic Performance Comparison of NACA 0012 and NACA 2412 Airfoils at Laminar Flow Condition," *Int. J. Multidiscip. Res.*, vol. 8, no. 1, p. 69250, Feb. 2026, doi: 10.36948/ijfmr.2026.v08i01.69250.

[14] M. F. Ali, N. Khan, W. Akram, and M. O. Qidwai, "Structural Design and CFD Analysis on Airfoil Model," *Glob. Sci-Tech*, vol. 13, no. 2, pp. 64–74, 2021, doi: 10.5958/2455-7110.2021.00009.4.

[15] Dr. S. Jabeen, "Computational Fluid Dynamics: Governing Equations and Numerical Techniques," *Int. J. Res. Sci. Innov.*, vol. 12, no. 12, pp. 1764–1772, 2026, doi: 10.51244/IJRSI.2025.12120149.

